Derivation of Fused-Sphere Molecular Surfaces from Properties of the Electrostatic Potential Distribution

QISHI DU and GUSTAVO A. ARTECA*

Département de Chimie et Biochimie, Laurentian University, Ramsey Lake Road, Sudbury, Ontario P3E 2C6, Canada

Received 12 July 1995; accepted 6 October 1995

ABSTRACT

The distribution of molecular electrostatic potential (MEP) on a surface is a common model used to describe simultaneously *steric* properties (e.g., size, shape) and *reactive* properties (e.g., electro- and nucleophilic positions) of a molecule. In this work, we analyze some relations between these two properties. In particular, we explore the possible definition of an optimum fused-sphere molecular surface from properties of the MEP distribution. With this goal, we study how several statistical descriptors of the two-dimensional MEP distribution change upon shrinking or enlarging a van der Waals surface. We find that some of the descriptors exhibit critical points in terms of a scaling factor. We use this property to define effective atomic radii. In particular, *we find that a reasonable molecular envelope is defined as the surface having the lowest (i.e., most negative) average negative MEP, with the largest possible dispersion about the mean.* We discuss the resulting atomic radii and compare them with others in the literature derived from only steric considerations. The present results expand the scope of fused-sphere surfaces for modeling microscopic or structural molecular properties.

Introduction

Current applications of quantitative structure–activity relations in molecular modeling rely heavily on evaluating microscopic properties such as surface area, volume, "shape," polarizability or lipophilicity.[1–4] Some of these properties require the definition of a molecular surface,[5,6] whereas others incorporate reactivity in addition to steric factors.[7] Molecular interactions, rather than molecular size, account for lipophilicity, drug recognition, ligand binding, as well as electrophilic and nucleophilic affinities. Most of these properties can be quantified by studying the molecular electrostatic potential (MEP) produced by a single species[8,9] or the interaction between several molecules.[10,11] As a result, a technique involving

*Author to whom all correspondence should be addressed.

CCC 0192-8651 / 96 / 101258-11

the *simultaneous* analysis of both surface and electrostatic properties provides an appealing model for rationalizing chemical regioselectivity[12,13] and some biochemical activities.[14,15]

Strategies for the practical computation[12,16] and characterization[15,17] of the interrelation between a molecular surface and its two-dimensional (2D) MEP distribution have been proposed in the literature. In the simplest approach, we can deal with a single molecule. Its molecular envelope can be represented as a fused-sphere van der Waals surface (VDWS) and its electrostatic potential evaluated from the electron density or effective atomic charges. This usual approach considers steric and electrostatic features as independent. In this case, the chosen molecular surface provides only the *support object* for the evaluation of MEP. In contrast, one could also adopt a unified view. One may pose the following questions: Is there a *special* or *natural* molecular surface for the computation of the electrostatic potential? Can we *define* the molecular surface from properties of the electrostatic potential distribution? In this work, we address this issue by analyzing the dependence of the 2D MEP distribution when the molecular surface is either enlarged or contracted.

There are several definitions in the literature for the atomic radii used in constructing fused-sphere molecular envelopes. Interatomic distances in condensed phase[18-22] and partial molecular volumes[23] provide estimations of atomic radii. Theoretical estimations are normally derived from single-molecule analyses. Atomic radii have been deduced from total electron isodensity contours, including their enclosed volume and curvature properties,[24,25] conformational invariances,[26] and approximations by localized Gaussian functions.[27]

The MEP has also been used to define atomic size. For instance, the covalent radius is found to be close to the distance at which the MEP of an isolated atom equals the chemical potential from density functional theory.[28] In the particular case of atomic anions, approximate radii have been defined as the distance from the nucleus to a negatively valued MEP minimum.[29-31] A similar principle has been used to analyze the size of molecular anions.[32] In addition, several *ad hoc* recipes have been proposed to "correct" the VDWSs of ions and neutral species by scaling to achieve better agreement with certain empirical properties.[33]

In line with the above results, we adopt here the viewpoint that the MEP distribution on a scalable VDWS leads to a useful molecular model. In this work, we show that a scale of effective atomic radii can be constructed from the critical points of the MEP distribution as a function of a scaling factor of the VDWS. We focus on *average and dispersion properties of the distribution* and *not* only special pointlike values such as MEP minima. (Note that the VDWS is *not* an equipotential surface. The MEP can have a complicated distribution on this surface.) Distribution descriptors on a *particular molecular surface* have been used recently by Politzer and coworkers to model partition coefficients.[2,4,34,35] Here, we analyze the behavior of the same descriptors over a *continuous variation of molecular surfaces*. As a result, we can re-examine the scales of atomic radii in terms of reactivity, in addition to steric factors.

The work is organized as follows. In the next section, we discuss some technical aspects of the computation of *ab initio* MEP over molecular surfaces and the statistical characterization of its distribution. The methodology is applied to scalable VDWSs of a number of small organic molecules. Following sections explore the dependence of the results on a number of factors, including the algorithm for generating the molecular surface, the molecular equilibrium geometry, and the basis set used for evaluating the MEP. Finally, we derive a scale of effective atomic radii and compare it with other results in the literature.

Computation of Electrostatic Potential on Molecular van der Waals Surfaces

The electrostatic potential $V(\mathbf{r})$ at a point $\mathbf{r}$ about a molecule has two contributions: one due to the nuclei (taken as classical point charges), and another associated with the electrons (treated quantum mechanically). The so-called "molecular electrostatic potential" (MEP) is expressed usually as an *electric potential energy*. For a molecule with n nuclei, this "potential" is written as (in atomic units):

$$V(\mathbf{r}) = \sum_{\alpha=1}^{n} \frac{Z_\alpha}{\|\mathbf{R}_\alpha - \mathbf{r}\|} - \sum_i \sum_j A_{ij} \int_\nu \phi_i^*(\mathbf{r}') \phi_j^*(\mathbf{r}') \frac{d\mathbf{r}'}{\|\mathbf{r}' - \mathbf{r}\|} \quad (1)$$

where Z_α is the charge on nucleus α (located at $\mathbf{R}_\alpha$), $\{\phi_i(\mathbf{r})\}$ is the set of atomic orbitals used to represent the electronic density function, and $\{A_{ij}\}$ the elements of the density matrix. The integral in

eq. (1) extends over the whole space v. In what follows, we give $V(\mathbf{r})$ in the standard units of kilocalories per mole.

For a number of molecules, we have computed the $V(\mathbf{r})$ function and the equilibrium nuclear geometries at *ab initio* level. The set of points $\{\mathbf{r}_k\}$ where the potential is evaluated are distributed on a van der Waals surface. Such a surface, indicated as $S_\rho(\mathbf{r})$, is the envelope defined by the interpenetration of atomic spheres, specified by a vector of atomic radii $\boldsymbol{\rho} = (\rho_1, \rho_2, \ldots, \rho_n)$. If we start from a surface $S_{\rho^0}(\mathbf{r})$ with radii $\boldsymbol{\rho}^0 = (\rho_1^0, \rho_2^0, \ldots, \rho_n^0)$, another surface with radii $\boldsymbol{\rho} = f\boldsymbol{\rho}^0$ will be said to be derived from $S_{\rho^0}(\mathbf{r})$ by a *uniform scaling*, with a scaling factor $f > 0$. Here, we study the MEP for these molecular surfaces. A similar approach to compute MEP on VDWSs was followed in Ref. 16.

In practice, the molecular surface is represented by a grid of points. We have considered two such point distributions: (i) the "Connolly surface,"[36,37] that produces a rather isotropic distribution with a desired density of points δ (measured in points/Å^2) at each atomic sphere; and (ii) the "Gepol surface,"[38] that is generated by a series of triangulations of a C_{60}-like polyhedron initially inscribed in each atomic sphere. A modification of the original Gaussian-80 (G80) program[39] allows the computation of the MEP on a Connolly surface generated internally.[40] We have adapted this modification to the computation of the present set of molecules; this approach will be referred to as G80M2 (Gaussian-80 Modification 2). For comparison, we have also computed the MEP on VDWSs, using the Gaussian-92 program[41] on grid surfaces generated separately with the MS program of Connolly[36,37] and Gepol program of Pascual-Ahuir et al.[38] We refer to these latter two approaches as G92/MS and G92/Gepol, respectively. The results of the three computational schemes are compared below for VDWSs with various numbers of grid points m.

Several statistical descriptors are used to characterize the MEP distribution on the molecular surface. We use the behavior of these descriptors with respect to scaling in order to select an effective molecular surface. Here, we employ the same descriptors studied in refs. 34 and 35:

$$\bar{V} = \frac{1}{m}\sum_{i=1}^{m} V(\mathbf{r}_i) \tag{2}$$

$$\Pi = \frac{1}{m}\sum_{i=1}^{m} |V(\mathbf{r}_i) - \bar{V}| \tag{3}$$

$$\bar{V}^- = \frac{1}{m_-}\sum_{i=1}^{m_-} V^-(\mathbf{r}_i),\ V^-(\mathbf{r}_i) < 0 \tag{4}$$

$$\bar{V}^+ = \frac{1}{m_+}\sum_{i=1}^{m_+} V^+(\mathbf{r}_i),\ V^+(\mathbf{r}_i) > 0 \tag{5}$$

$$\sigma_-^2 = \frac{1}{m_-}\sum_{i=1}^{m_-} \left[V^-(\mathbf{r}_i) - \bar{V}^-\right]^2,\ V^-(\mathbf{r}_i) < 0 \tag{6}$$

$$\sigma_+^2 = \frac{1}{m_+}\sum_{i=1}^{m_+} \left[V^+(\mathbf{r}_i) - \bar{V}^+\right]^2,\ V^+(\mathbf{r}_i) > 0 \tag{7}$$

$$\sigma_t^2 = \sigma_+^2 + \sigma_-^2 \tag{8}$$

$$\nu = \frac{\sigma_+^2\sigma_-^2}{\left[\sigma_t^2\right]^2} \tag{9}$$

which are, respectively: eq. (2), the mean MEP value over the entire surface; eq. (3), the deviation in absolute value from the mean; eq. (4), the mean *negative* MEP value on the surface (i.e., the average including only the m_- grid points on the VDWS with $V(\mathbf{r}_k) < 0$); eq. (5), the mean *positive* MEP value on the surface (i.e., the mean including only the m_+ grid points on the VDWS with $V(\mathbf{r}_k) > 0$); eq. (6), the standard deviation over the negative MEP regions of the surface; eq. (7), the standard deviation over the positive MEP regions of the surface; eq. (8), the total MEP dispersion on the surface; and eq. (9), the so-called "balance parameter," which measures the asymmetry in the dispersions σ_-^2 and σ_+^2 of MEP values. In addition, we have also studied mean MEP values and standard deviations on selected atoms. The notation $\bar{V}_A$ will indicate a mean computed with grid points only on atom A. Finally, we have also analyzed the absolute minimum and maximum MEP values on the surface (*min V* and *max V*, respectively).

We have computed the above descriptors for a number of molecules. We have tested molecular surfaces of various qualities and several *ab initio* schemes to compute the MEP.

First, we illustrate how the three methods compare with respect to the type of surface used. As an example, we show the results for a VDWS of furane (C_4H_4O), constructed with the atomic radii given in Ref. 23. Tables I and II show the results for the MEP distribution calculated at the *ab initio* RHF/STO-5G level, at an equilibrium geometry optimized within the same framework. (This rather unusual basis set is used here only to facilitate comparisons with the literature. This is the basis set employed in Refs. 34 and 35 for evaluating statistical descriptors on isodensity contours of various molecules.) Tables I and II convey the

TABLE I.
Properties of the MEP Distribution on the Molecular Surface of C_4H_4O, Using Different Computational Approaches.[a]

Method	m	$min\,V$	$max\,V$	$\bar{V}_O$	$\bar{V}_C$	$\bar{V}_H$
G80M2	1136	−33.413	19.171	−21.631	0.0251	14.515
G80M2	1422	−33.326	19.187	−21.838	0.0251	14.376
G80M2	1507	−33.326	19.200	−21.838	0.0251	14.364
G92 / MS	2080	−33.443	19.190	−20.330	−0.3765	14.370
G92 / MS	2391	−33.451	19.199	−21.204	−0.2447	14.370
G92 / MS	2935	−33.452	19.176	−21.587	−0.2447	14.420
G92 / Gepol	307	−33.292	19.027	−21.852	0.3640	13.680

[a] In the approaches coded G80M2 and G92 / MS, the number of points m on the surface is regulated by a quasi-isotropic distribution of points with a given surface density. In the case of G92 / Gepol, the number of points is determined by a level of subtriangulation in a polyhedron initially inscribed into an atomic sphere. Computations are at *ab initio* RHF / STO-5G level, on the STO-5G optimized geometry. All MEP values are given in kilocalories per mole.

reliability of the MEP descriptors. From Table I, we observe that:

(i) G80M2 and G92/MS give similar, yet not coincident, values. This can be attributed to the fact that a choice of different molecular orientation produces a different surface grid.

(ii) The results indicate that a density of points of $\delta \approx 25$ pts/Å^2 on a Connolly surface is sufficient for most computations. Note that a much smaller number of points is needed when using Gepol.

(iii) The MEP averaged over atoms confirms that O is the most electronegative (lowest or most negative MEP) and H the more electropositive (highest MEP). The errors in $\bar{V}_C$ are magnified because it is close to zero.

Table II indicates that the descriptors computed most accurately are Π, $\bar{V}^-$, and σ_+^2, followed by $\bar{V}^+$ and σ_-^2. Note that, with the definitions in eqs. (2), (4), and (5), the negative and positive MEP averages do not add up to $\bar{V}$. The actual addition takes the form $\bar{V} = (m_-/m)\bar{V}^- + (m_+/m)\bar{V}^+$.

We have also noted only a small dependence of these results on minor changes in the equilibrium geometry, such as those caused by reoptimization with a different basis set. This observation is valid for all other molecules studied in this work. The dependence on the computational strategy to evaluate the MEP is discussed in the next section, in relation to the scaling of molecular surfaces.

Dependence of MEP Distribution on Isotropic Scaling of an Initial Molecular Surface

In this section, we consider seven planar molecules, namely C_4H_4O, C_6H_5OH, C_5H_5N, C_6H_6, C_6H_5F, C_6H_5Cl, and $C_6H_5NH_2$. These

TABLE II.
Statistical Descriptors of the MEP Distribution on the Molecular Surface of C_4H_4O, Using Different Approaches.[a]

Method	m	Π	$\bar{V}$	$\bar{V}^+$	$\bar{V}^-$	σ_+^2	σ_-^2	σ_t^2	ν
G80M2	1136	8.607	1.522	9.288	−7.909	28.73	68.35	97.08	0.208
G80M2	1422	9.233	3.033	10.294	−8.720	25.91	77.41	103.32	0.188
G80M2	1507	9.199	3.588	10.522	−8.720	24.95	77.43	102.38	0.184
G92 / MS	2080	8.145	1.292	8.863	−7.339	29.73	59.55	89.27	0.222
G92 / MS	2391	8.521	1.443	9.230	−7.773	28.98	65.52	94.51	0.213
G92 / MS	2935	9.257	2.676	10.186	−8.701	26.56	77.27	103.83	0.190
G92 / Gepol	307	8.076	2.971	9.088	−7.681	24.71	59.31	84.02	0.208

[a] See Table I for the computational details. MEP values in kilocalories per mole.

molecules will be used for a rough estimation of the effective radii of the electronegative atoms O, N, F, and Cl. The analysis of C and H atoms is discussed in the next section, by using a number of hydrocarbons.

The geometries of all seven molecules have been optimized with G92 at the level of STO-5G. Three basis sets, STO-5G, 4-31G, and 6-31G*, are used in the calculations of MEP. For C_6H_5Cl, the MEP calculations on the molecular surfaces are performed with the G92/MS method, using the 6-31G* basis set and a surface density of $\delta = 50$ points/Å^2. All other MEP calculations on molecular surfaces are performed with the scheme G80M2. (In this latter case, the surface areas are smaller, and we have used a density of $\delta = 25$ points/Å^2.)

At this point, we are interested in establishing the behavior of MEP descriptors with respect to a surface defined from a vector of "standard" atomic radii $\boldsymbol{\rho}^0$. The change in surface is determined by a single scaling parameter f. With this parameter, a surface will change from $\boldsymbol{\rho}^0$ to $\boldsymbol{\rho} = f\boldsymbol{\rho}^0$. At present, we shall simply choose the standard $\boldsymbol{\rho}^0$ given by the radii in Ref. 23. [For the molecules in this work, these standard values are (in ångströms): $\rho_H^0 = 1.17$, $\rho_C^0 = 1.75$, $\rho_N^0 = 1.55$, $\rho_O^0 = 1.40$, $\rho_F^0 = 1.35$, and $\rho_{Cl}^0 = 1.85$.] These radii, derived from molecular volume measurements, are commonly employed in the literature. For the moment, these radii carry no meaning with respect to the MEP distribution. We can now test how some statistical descriptors, such as $\bar{V}^-$ and $\bar{V}$, change upon scaling the reference surface $\boldsymbol{\rho}^0$. In a later section, we discuss an approach that bypasses the choice of a standard $\boldsymbol{\rho}^0$.

First, we illustrate the effect of the basis set on the MEP distribution for scaled VDWSs. Figures 1 and 2 show the results for C_6H_5OH. Figure 1 displays the change of the absolute MEP minimum on the molecular surface as a function of the scaling parameter. We observe two clear features: (i) regardless of the basis set used to computed the MEP, *min V* presents a unique minimum ([*min V*]*) at a value f^*:

$$[\,min\,V\,]^* = \min_{\{f\}}\left[\min_{\{\mathbf{r}\}} V(\mathbf{r})\right] \qquad (10)$$

and (ii) the actual position and value of the minimum depend on the basis set. The lowest *min V* value (i.e., the most negative) with the STO-5G basis takes place at a rather small VDWS ($f^*_{\text{STO-5G}} \approx 0.70$). The position f^* of the minima for the basis sets 4-31G and 6-31G* are closer ($f^*_{\text{4-31G}} \approx$

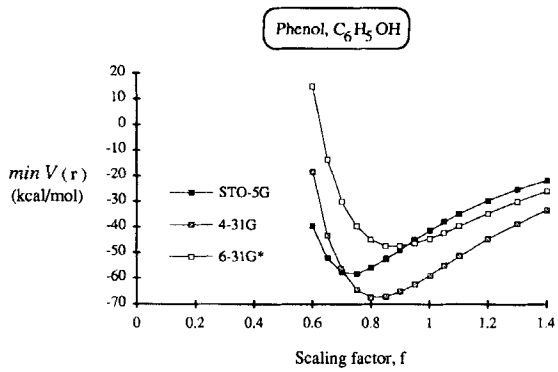

FIGURE 1. Dependence of the MEP minimum [*min V*(**r**)] with respect to scaling in the VDWS of phenol (C_6H_5OH). [The *ab initio* MEP are computed with different basis sets. The initial ($f = 1$) surface is defined by the radii in ref. 23. Nuclear geometries are optimized at RHF / STO-5G level.]

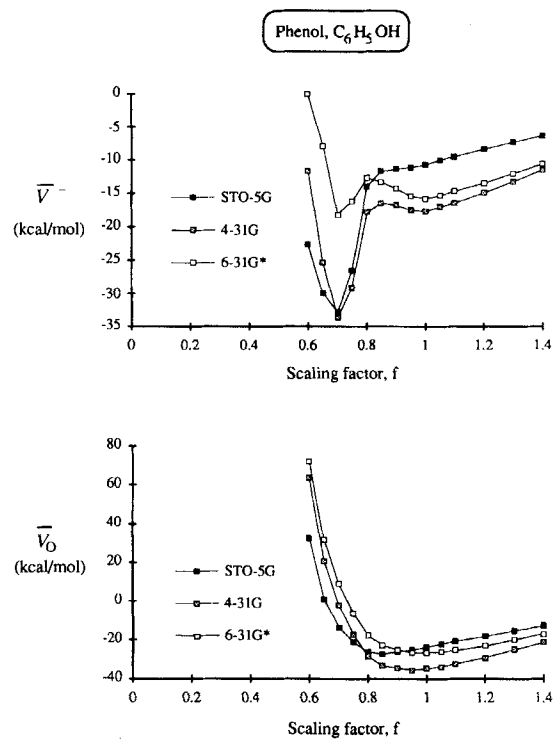

FIGURE 2. Dependence of the mean negative MEP ($\bar{V}^-$) and mean MEP on the oxygen atomic sphere ($\bar{V}_O$) with the scaling of the VDWS of phenol (C_6H_5OH). [The *ab initio* MEP computed with different basis sets are evaluated on a VDWS defined by the radii in ref. 23. Nuclear geometries are optimized at RHF / STO-5G level. Note that $\bar{V}^-$ vs. f exhibits two minima correlating with the approximate positions of inner and outer electron shells.

0.85, $f^*_{6\text{-}31G^*} \approx 0.90$), even though their $[min\,V]^*$ values are rather different. Note that, as the basis set improves, the optimum scaling parameter f^* moves closer to $f^* \approx 1$. In other words, the surface defined by the VDWS with the smallest $min\,V$ value would appear to be similar to the molecular envelopes built so as to fit the experimental volume per molecule (the "actual" molecular size defined by the reference vector $\boldsymbol{\rho}^0$).

Figure 2 complements the analysis by presenting descriptors of MEP averaged over the surface, instead of single-point values. The figure shows the mean negative potential on the surface ($\overline{V}^-$, top) and the mean MEP on the "exposed" surface of the most electronegative atom ($\overline{V}_0$, bottom). From Figure 2, we extract the following information:

(i) The $\overline{V}^-$ presents two minima as a function of f, except when using the STO-5G basis set. The position of one minimum is virtually coincident in all cases ($f^* \approx 0.70$). This minimum defines a very compact VDWS, corresponding to the high-electron-density region. Since the minimal basis set is known to describe poorly the low density regions (outer electron shells), we can assume that the first minimum is not relevant to realistic molecular surfaces. The second minimum, $[\overline{V}^-]^*$, defines a VDWS close to the surface taken as a reference ($f^*_{4\text{-}31G} \approx f^*_{6\text{-}31G^*} \approx 1$). (This second minimum is not observed in the calculations with the STO-5G basis set.)

(ii) The average MEP over the oxygen atom, $\overline{V}_O$, exhibits a similar behavior to $min\,V$, although its associated minimum is closer to the second minimum of $\overline{V}^-$. The minima are specified by $f^*_{STO\text{-}5G} \approx 0.85$, $f^*_{4\text{-}31G} \approx 0.95$, and $f^*_{6\text{-}31G^*} \approx 1.0$.

These observations indicate again that the scaled molecular surface that produces an absolute minimum in one of the MEP descriptors is not far from a "standard" (empirical) VDWS. The results indicate that the STO-5G basis is not adequate for the analysis because it produces a too compact molecular envelope. These features are also encountered for other molecules studied in the present work.

Table III shows in more detail the behavior of a number of descriptors over a scaled molecular surface. The example chosen for illustration is furane (C_4H_4O), where the MEP is computed at the *ab initio* level with the 6-31G* basis set. Table III shows the variation of the $min\,V$ and $max\,V$ on the surface as a function of the scaling parameter. (The atomic sphere where the critical point is located is also indicated.) As expected, $min\,V$ is located on the exposed surface of the most electronegative atom (O), whereas the location of the maximum changes from O to C and to H as the surface enlarges. Note that $min\,V$ exhibits an absolute minimum, $[min\,V]^*$, as a function of f (at $f^* \approx 0.90$), whereas $max\,V$ decreases monotonically with f.

Table III illustrates another property we observed throughout: the MEP averaged over the surface of one atom, $\overline{V}_A$, exhibits an absolute minimum as a function of f *as long as* $\overline{V}_A$ *is negative*, $\overline{V}_A < 0$. The location of the minima for $\overline{V}_O$ and $\overline{V}_C$ are found at $f^* \approx 1.0$ and $f^* \approx 1.1$, respectively.

Table IV expands the previous analysis to all remaining MEP descriptors. The only descriptors that exhibit extrema upon scaling are $\overline{V}^-$, σ^2_-, and ν. In the first case, we find a minimum $[\overline{V}^-]^*$ close to the standard VDWS ($f^* \approx 1.0$). (It should be noted that $\overline{V}^-$ is computed over a portion of the surface *that includes several atoms and not only the oxygen.*) In the case of the other two parameters (σ^2_-, and ν), we find a *maximum* associated with a more compact surface ($f^* \approx 0.85$).

In summary, Tables III and IV establish that the regions with negative MEP are the relevant ones for the definition of a molecular surface. Both the average negative potential $\overline{V}^-$ and its dispersion σ^2_-, as well as the averages over electronegative atoms, present critical points as a function of the scaling parameter f. (Note that the average, such as $\overline{V}_A$, exhibits such a behavior *only* if it is negative.)

These observations are valid for all other molecules we have analyzed. Figure 3 collects the results of $min\,V$ over the scaled VDWSs of the seven molecules, using the 6-31G* basis set. In all cases we find a single critical point, although its position f^* depends on the most electronegative atom present. Figure 4 displays the results for $\overline{V}^-$ and $\overline{V}_A$ (with "A" being the most electronegative element present). The conclusions derived are similar to those extracted from Figure 2: *all surfaces present one local minimum* $[\overline{V}^-]^*$ *and the global minimum* $[\overline{V}_A]^*$ *at a value not far from* $f^* \sim 1.0$. From the condition to have negative MEP on the surface of the most electronegative atom ($\overline{V}_A < 0$) we can establish a lower bound for the scaling factor, $f > 0.70$.

TABLE III.

MEP Distribution on the Surface of C_4H_4O Calculated at the *Ab Initio* 6-31G* Level, With a Density of 25 Pts / Å^2, Using the G80M2 Method.[a]

f	$min\,V$	Atom (min)	$max\,V$	Atom (max)	$\bar{V}_0$	$\bar{V}_C$	$\bar{V}_H$
0.60	26.161	O	256.158	O	86.61	72.34	78.74
0.70	−18.950	O	118.725	C	15.69	27.30	49.06
0.75	−29.468	O	73.612	C	0.68	24.53	45.87
0.80	−35.362	O	52.515	C	−12.05	7.83	33.20
0.85	−37.968	O	39.358	H	−19.84	3.08	27.93
0.90	−38.543	O	34.427	H	−21.60	−0.01	23.92
0.95	−38.007	O	30.380	H	−25.96	−2.02	20.82
1.00	−36.673	O	27.013	H	−26.07	−2.94	18.42
1.05	−34.870	O	24.179	H	−25.77	−3.50	16.39
1.10	−32.826	O	21.789	H	−24.81	−3.56	14.81
1.20	−28.578	O	18.017	H	−23.63	−2.46	12.57
1.30	−24.623	O	15.188	H	−20.75	−1.80	10.89
1.40	−21.199	O	13.001	H	−18.08	−0.99	9.81

[a]The potential is evaluated at the RHF / STO-5G optimized geometry. MEP values in kilocalories per mole. The "Atom" columns identify the exposed atomic sphere where the critical point is located.

Table V collects our rough estimations of the critical scaling factor f^* associated with the critical points in $min\,V$, $\bar{V}_A$, $\bar{V}^-$, and σ_-^2 over the continuum of VDWSs defined from the standard surface ρ^0. For the series of molecules in this section, we find:

$$f^*(min\,V) \approx 0.91 \pm 0.12; \quad f^*(\bar{V}_A) \approx 0.98 \pm 0.09;$$
$$f^*(\bar{V}^-) \approx 1.01 \pm 0.09; \quad f^*(\sigma_-^2) \approx 0.91 \pm 0.17 \tag{11}$$

These results indicate that the "critical" molecular surface, defined with the radii vector $\rho^* = f^*\rho^0$, is indeed very similar to the standard VDWS defined with the radii in ref. 23.

The findings discussed in this section can be summarized as follows: a fused-sphere surface leads to critical points in various 2D descriptors of negative MEP when the surface is not far from "standard" molecular envelopes. In other words, a VDWS can be associated not only with an "experimental" molecular volume but also with a region

TABLE IV.

Statistical Descriptors of the MEP Distribution on the VDWS of C_4H_4O Given in Terms of the Scaling Factor f.[a]

f	Π	$\bar{V}$	$\bar{V}^+$	$\bar{V}^-$	σ_+^2	σ_-^2	σ_t^2	ν
0.60	18.973	81.955	81.995	0.000	845.89	0.00	845.89	0.000
0.70	16.427	37.320	38.922	−9.972	327.86	33.84	361.70	0.085
0.75	16.381	25.573	30.008	−9.636	231.45	80.39	311.84	0.191
0.80	16.608	17.578	25.270	−11.148	166.78	92.03	258.82	0.229
0.85	16.554	12.445	22.815	−12.027	115.22	101.92	217.14	0.249
0.90	16.216	8.784	20.434	−13.242	83.94	99.93	183.87	0.248
0.95	15.497	6.712	18.445	−13.929	59.78	95.19	154.97	0.237
1.00	14.595	5.457	16.596	−14.221	45.17	86.74	131.91	0.225
1.05	13.706	4.498	15.098	−13.924	34.88	79.19	114.06	0.212
1.10	12.914	3.309	13.591	−13.534	28.47	70.39	98.86	0.205
1.20	11.077	2.272	11.198	−12.013	20.15	57.48	77.63	0.192
1.30	9.664	1.362	9.394	−10.624	15.26	44.03	59.29	0.191
1.40	8.441	0.675	8.012	−9.224	11.59	33.96	45.55	0.190

[a]The potential is evaluated at *ab initio* 6-31G* level with the RHF / STO-5G optimized geometry, on a surface with a density of 25 pts / Å^2. MEP values are in kilocalories per mole.

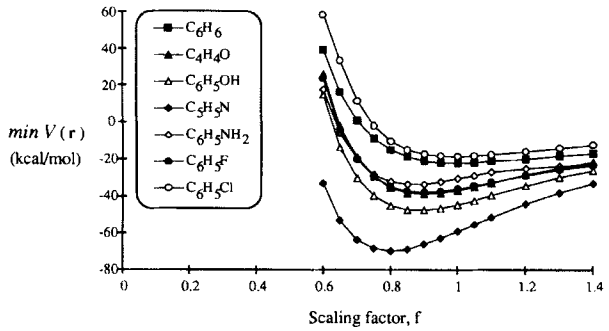

FIGURE 3. Dependence of the MEP minimum [*min* $V(\mathbf{r})$] with respect to scaling in the VDWS of seven aromatic compounds (benzene, furane, phenol, pyridine, aniline, fluorobenzene, and chlorobenzene). [The MEP is computed at *ab initio* RHF / 6-31G* level, with nuclear geometries optimized at the RHF / STO-5G level. The initial ($f = 1$) surface is defined by the radii in ref. 23.]

of space where the molecule exhibits its most negative ("lowest") average negative MEP, together with its maximum dispersion about the mean. This property of the MEP indicates that the surface obtained defines the space leading to the largest stabilization of an attacking electrophilic group.

MEP Distribution on Molecular Surface of Small Hydrocarbons

The analysis in the previous section can be extended by studying the behavior of the descriptors *min* V, $\bar{V}_A$, $\bar{V}^-$, and σ_-^2 as continuous functions of the atomic radii ρ_i. This is a more demanding approach, as the 2D MEP becomes a function on as many variables as distinct nuclei in the molecule. In this section, we carry out one analysis restricted to the case of only two distinct atomic radii.

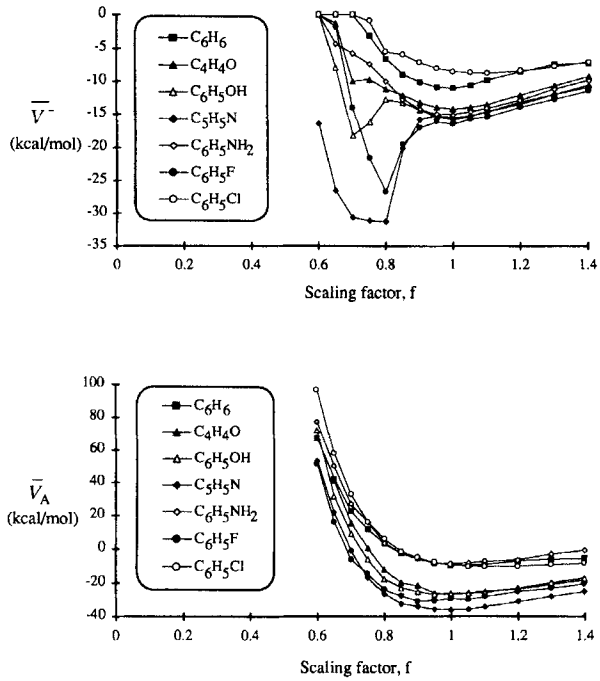

FIGURE 4. Scaling dependence of the mean negative MEP ($\bar{V}^-$) and mean MEP on the atomic sphere with the most-electronegative atom ($\bar{V}_A$) for various molecules. [For the list of molecules in Fig. 3, the electronegative atoms A are C, O, O, N, N, F, and Cl, respectively. The MEP is computed at *ab initio* RHF / 6-31G* level, with nuclear geometries optimized at the RHF / STO-5G level. Note that all minima for the "outer shell" take place at a scaling parameter close to the initial VDWS, $f \approx 1$.]

As illustrative examples, we have studied the behavior of the MEP descriptors in a number of representative small hydrocarbons: CH_4, C_2H_5,

TABLE V.
Critical Points in the MEP Descriptors for Various Molecules.

Molecule	$f^*(min\,V)$	$[min\,V]^*$	$f^*(\bar{V}_A)$	$[\bar{V}_A]^*$	$f^*(\bar{V}^-)$	$[\bar{V}^-]^*$	$f^*(\sigma_-^2)$	$[\sigma_-^2]^*$
C_6H_6	1.00	−22.01	1.00	−9.66	1.00	−11.032	1.10	39.121
C_4H_4O	0.90	−38.54	1.00	−26.07	1.00	−14.221	0.85	101.924
C_6H_5OH	0.90	−47.34	0.95	−26.71	1.00	−15.780	0.75	203.693
C_5H_5N	0.80	−69.68	1.00	−35.90	1.00	−15.539	0.85	434.459
$C_6H_5NH_2$	0.85	−33.54	1.00	−8.64	1.00	−15.034	1.00	61.505
C_6H_5F	0.90	−37.65	0.90	−30.69	1.00	−16.444	0.85	215.600
C_6H_5Cl	1.00	−18.54	1.10	−10.32	1.10	−8.760	0.95	24.273

[a]The values of the scaling parameter f where the critical points are found are indicated by f^* (with an uncertainty of ± 0.05). All results correspond to RHF / 6-31G* potentials computed at the RHF / STO-5G optimized conformations. MEP values are in kilocalories per mole. The isotropic scaling is performed on the VDWS defined with the radii given in Ref. 23. A density of points $\delta = 25$ points / Å^2 is used, except for C_6H_5Cl which was calculated with $\delta = 50$ points / Å^2.

C_2H_4, C_2H_2, and C_6H_6. In these cases, the MEP descriptors depend only on the radii of carbon and hydrogen, ρ_C and ρ_H, respectively.

Figure 5 shows the dependence of *min V* in terms of ρ_C and ρ_H, for ethane and benzene. For a given value of ρ_H, we notice a minimum in the descriptor *min V* as a function of ρ_C. In contrast, *min V* appears quite insensitive to ρ_H, for values ranging from 0.9 to 1.6 Å. Within this range, we observe a single absolute minimum [*min V*]* positioned at $\rho_C \sim 2.0$ Å for ethane, and $\rho_C \sim 1.8$ Å for benzene. The same qualitative behavior is found for the other hydrocarbons.

Above result indicates that the hydrogen atom is rather "invisible" in the MEP distribution. This feature is not unexpected considering its low electron density. A similar situation is found experimentally in X-ray diffraction, where the electron density about the hydrogen atoms cannot be detected. This insensitivity of the MEP distribution makes it difficult to make an estimation of the optimum value ρ_H^*. This observation agrees with the fact that the largest discrepancies in the literature on atomic radii are found for hydrogen, with values ranging from 1.0 to 1.3 Å.[18,19,23,42] Other MEP descriptors exhibit a comparable behavior, even though the degree of their dependence on ρ_H varies. Figure 6 shows $\overline{V}^-$ as a function of ρ_C and ρ_H for ethane and benzene. Qualitatively, we observe the same behavior as in Figure 5: the minima of $\overline{V}^-$ appear at $\rho_C \sim 2.0$ Å for ethane and $\rho_C \sim 1.8$ Å for benzene. However, the insensitivity on the ρ_H value is less marked. For both molecules, we notice a rapid rise in $\overline{V}^-$ for $\rho_H > 1.3$ Å. Therefore, a reasonable upper bound to the atomic radius of hydrogen can be extracted from $\overline{V}^-$, although not an optimum value. A similar result for this descriptor is observed in the other hydrocarbons.

In summary, an analysis of 2D MEP descriptors as *continuous functions of the atomic radii* indicates the occurrence of molecular surfaces where these descriptors present critical points. This result coincides with the observations made in previous sections for *scaled* fused-sphere surfaces.

Using the above analysis, we can extract optimum atomic radii for carbon atoms in various

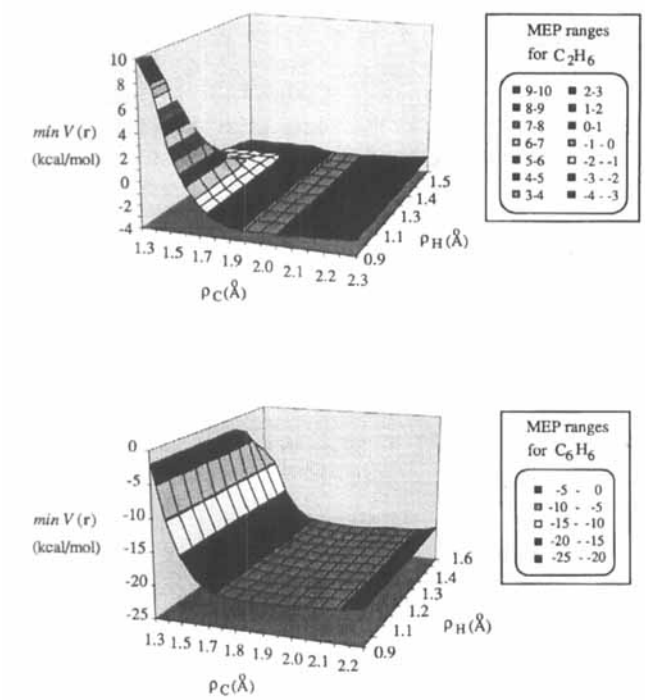

FIGURE 5. Scaling dependence of the absolute MEP minimum on VDWSs of ethane and benzene. [The MEP is computed at *ab initio* RHF / 6-31G* level, with nuclear geometries optimized at the RHF / STO-5G level. The molecular surfaces are generated by continuous variation of both C and H atomic radii. Note that ρ_H appears to have little role on the values of *min V*(**r**).]

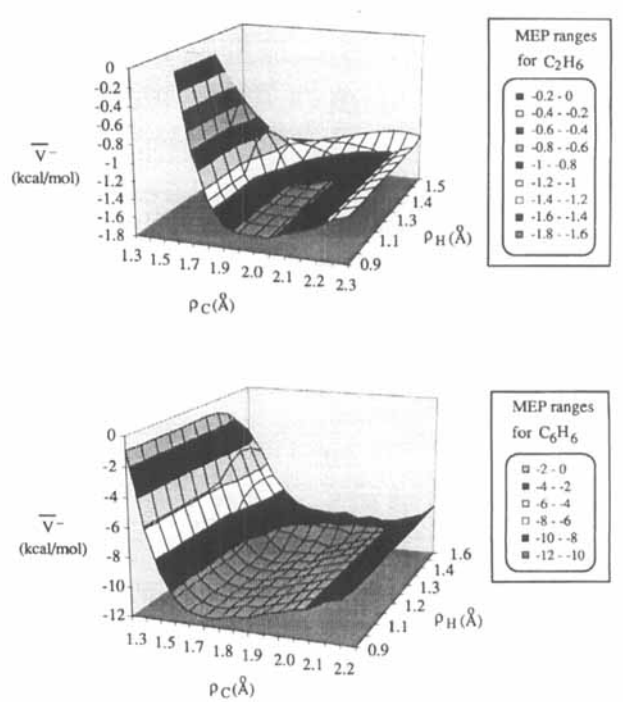

FIGURE 6. Scaling dependence of the mean negative MEP on VDWSs of ethane and benzene. [The MEP is computed at *ab initio* RHF / 6-31G* level, with nuclear geometries optimized at the RHF / STO-5G level. The molecular surfaces are generated by continuous variation of both C and H atomic radii. The descriptor $\overline{V}^-$ exhibits some dependence on the ρ_H values (cf. Fig. 5).]

compounds. (In contrast, our approach is not sensitive enough to provide anything but a *range* of values for the atomic radius of hydrogen.) The study of hydrocarbons indicates that the optimum value ρ_C^* depends on the "type" of carbon atom (i.e., its hybridization scheme). Our estimations are summarized in Table VI. These values are derived by using several MEP descriptors and a fixed atomic radius for hydrogen (ρ_H = 1.17 Å).[23] The values for ρ_C^* vary from 2.00 to 1.65 Å when changing from sp^3 to sp hybridization. The result from benzene provides a radius for aromatic carbon of 1.77 Å, comprised between those of sp^3 and sp^2 carbons. These atomic radii are close to those derived in the previous section by scaling molecular surfaces. In that case, we found a scaling factor f^* close to unity when using a standard radius of 1.75 Å for carbon.

These present hybridization-dependent values of ρ_C^* agree well with others in the literature.[19-23] Nevertheless, we point out again that this agreement is nontrivial: our radii are extracted from the critical behavior of the electrostatic potential and *not* from molecular volume or molecular interaction considerations.

We expect that the coincidence between the optimum radii derived in this section and the radii derived by simply scaling a reference VDWS should also be maintained for elements other than carbon.

Conclusions

In this work, we have shown the occurrence of critical points in a number of descriptors of the electrostatic potential distribution on molecular surfaces. These extrema appear when the descriptors are analyzed over a continuum of molecular surfaces. In our case, we find that 2D descriptors associated with the negative MEP can be used to derive optimum atomic radii. These radii define a region of space about a molecule in terms of reactivity properties rather than only stericity or molecular volume. In particular, the surface can be chosen as the one leading to the *maximum average stabilization of an attacking electrophile* (e.g., the surface with the most negative average potential $\bar{V}^-$).

Table VI summarizes our estimations of optimum atomic radii from the critical points on 2D MEP descriptors. The results for C are extracted from our analysis of hydrocarbons, whereas the results for heteroatoms are derived from the scaled VDWSs. The results are rough estimations based on a small number of molecules. However, the coincidence with other values in the literature, based on different principles, suggests that a more detailed study would not change the radii dramatically.

Finally, our results give some constraints on the quality of the basis set required to retain the correct features of the 2D MEP distribution. Note that a basis set with a poor behavior in the low-density regime (e.g., the STO-5G basis) fails at producing a second minimum in $\bar{V}^-$, as a function of factor scaling the molecular surface.

The present findings extend previous results in the literature. Earlier works have indicated that minima of the MEP function of atoms and atomic ions take place at distances comparable to covalent and ionic radii.[28-31] In this work, we have shown that this approach can be generalized to the case of model molecular surfaces: *we find that atomic radii for neutral molecules can be determined from the extrema of descriptors associated with the negative MEP on molecular surfaces.* The recommended descriptors are the averaged negative MEP on the surface, its deviation about the mean, and the averaged MEP on the exposed surface of the most electronegative atoms.

TABLE VI.
Selection of Atomic Radii (in Å) Based on MEP and Scaling of VDWSs.[a]

Atom	$\rho[min\, V_A]$	$\rho[\bar{V}_A]$	$\rho[\bar{V}^-]$	Estimate
C(sp^3)	2.00	2.00	2.00	2.00
C(aromatic)	1.80	1.75	1.75	1.77
C(sp^2)	1.70	1.70	1.70	1.70
C(sp)	1.60	1.65	1.70	1.65
N	1.28	1.55	1.55	1.46
O	1.26	1.37	1.55	1.39
F	1.22	1.22	1.35	1.26
Cl	1.85	2.03	2.03	1.97

[a]All atomic radii are derived from surfaces where the H radius is fixed at 1.17 Å.[23] The "estimates" only have ca. 10% accuracy.

Acknowledgments

The authors thank N. D. Grant (Sudbury) for her comments on the manuscript. This work has been supported by the Fonds de Recherche de l'Université Laurentienne (FRUL) and by an oper-

ating research grant from the Natural Sciences and Engineering Research Council (NSERC) of Canada.

References

1. M. H. Abraham, P. L. Grellier, J. M. Abboud, R. M. Doherty, and R. W. Taft, *Can. J. Chem.*, **66,** 2673 (1988).
2. J. S. Murray and P. Politzer, *J. Org. Chem.*, **56,** 6715 (1991).
3. G. H. Loew, H. O. Villar, and I. Alkorta, *Pharm. Res.* **10,** 475 (1993).
4. J. S. Murray, T. Brinck, P. Lane, K. Paulsen, and P. Politzer, *J. Mol. Struct. (Theochem)*, **307,** 55 (1994).
5. F. M. Richards, *Annu. Rev. Biophys. Bioeng.*, **6,** 151 (1977).
6. P. G. Mezey, *Reviews in Computational Chemistry*, vol. 1, K. B. Lipkowitz and D. B. Boyd, Eds., VCH, New York, 1990.
7. M. A. Johnson and G. M. Maggiora, Eds., *Concepts and Applications of Molecular Similarity*, Wiley, New York, 1990.
8. E. Scrocco and J. Tomasi, *Topics Curr. Chem.*, **42,** 95 (1973).
9. P. Politzer, D. G. Truhlar, Eds. *Chemical Applications of Atomic and Molecular Electrostatics*, Plenum, New York, 1981.
10. S. Miertuš, E. Scrocco, and J. Tomasi, *Chem. Phys.*, **55,** 117 (1981).
11. J. Israelachvili, *Intermolecular and Surface Forces*, Academic Press, London, 1992.
12. S. D. Kahn, C. F. Pau, L. E. Overman, and W. J. Hehre, *J. Am. Chem. Soc.*, **108,** 7381 (1986).
13. X. Luo, G. A. Arteca, P. G. Mezey, and C.-H. Zhang, *J. Organomet. Chem.*, **444,** 131 (1993).
14. G. A. Arteca, V. B. Jammal, P. G. Mezey, J. S. Yadav, M. A. Hermsmeier, and T. M. Gund, *J. Mol. Graph.*, **6,** 45 (1988).
15. G. A. Arteca, A. Hernández-Laguna, J. J. Rández, Y. G. Smeyers, and P. G. Mezey, *J. Comput. Chem.*, **12,** 705 (1991).
16. I. Alkorta, H. O. Villar, and G. A. Arteca, *J. Comput. Chem.*, **14,** 530 (1993).
17. P. G. Mezey, *Int. J. Quantum Chem., QBS*, **12,** 113 (1986).
18. L. Pauling, *The Nature of the Chemical Bond*, Cornell University, Ithaca, NY, 1960.
19. A. Bondi, *Physical Properties of Molecular Crystals, Liquids, and Glasses*, Wiley, New York, 1968.
20. L. S. Bartell, *J. Chem. Educ.*, **45,** 754 (1968).
21. C. Glidewell, *Inorg. Chim. Acta*, **12,** 219 (1975).
22. J. K. Burdett, *Molecular Shapes (Theoretical Models of Inorganic Stereochemistry)*, Wiley, New York, 1980.
23. A. Gavezzotti, *J. Am. Chem. Soc.*, **105,** 5220 (1985).
24. R. F. W. Bader, M. T. Carroll, J. R. Cheeseman, and C. J. Chang, *J. Am. Chem. Soc.*, **109,** 7968 (1987).
25. M. M. Francl, R. F. Houk, and W. J. Hehre, *J. Am. Chem. Soc.*, **106,** 563 (1984).
26. G. A. Arteca, N. D. Grant, and P. G. Mezey, *J. Comput. Chem.*, **12,** 1198 (1991).
27. J. A. Grant and B. T. Pickup, *J. Phys. Chem.*, **99,** 3503 (1995).
28. P. Politzer, R. G. Parr, and D. R. Murphy, *J. Chem. Phys.*, **79,** 3859 (1983).
29. K. D. Sen and P. Politzer, *J. Chem. Phys.*, **90,** 4370 (1989); ibid., **91,** 5123 (1989).
30. R. K. Pathak and S. R. Gadre, *J. Chem. Phys.*, **93,** 1770 (1990).
31. S. R. Gadre, I. H. Shrivastava, and S. A. Kulkarni, *Chem. Phys. Lett.*, **170,** 271 (1990).
32. S. R. Gadre, C. Kölmel, and I. H. Shrivastava, *Inorg. Chem.*, **31,** 2281 (1992).
33. F. J. Luque, S. R. Gadre, P. K. Bhadane, and M. Orozco, *Chem. Phys. Lett.*, **232,** 509 (1995).
34. P. Polizer, P. Lane, J. S. Murray, and T. Brinck, *J. Phys. Chem.*, **96,** 7938 (1992).
35. J. S. Murray, P. Lane, T. Brinck, and P. Polizer, *J. Phys. Chem.*, **97,** 5144 (1993).
36. M. L. Connolly, *Science*, **221,** 709 (1983).
37. M. L. Connolly, *J. Appl. Crystallog.*, **16,** 548 (1983).
38. J. L. Pascual-Ahuir, E. Silla, J. Tomasi, and R. Bonaccorsi, *J. Comput. Chem.*, **8,** 778 (1987).
39. *Gaussian 80*, J. S. Binkley, R. A. Whiteside, R. Krishnan, R. Seeger, D. J. Defrees, H. B. Schlegel, S. Topiol, L. R. Kahn, and J. A. Pople, Carnegie-Mellon University, Pittsburgh, PA, 1980.
40. U. C. Singh and P. A. Kollman, QPCE Program 446, Bloomington, IN, 1982.
41. M. J. Frisch, G. W. Trucks, M. Head-Gordon, P. M. W. Gill, M. W. Wong, J. B. Foresman, B. G. Johnson, H. B. Schlegel, M. A. Robb, E. S. Replogle, R. Gomperts, J. L. Andrés, K. Raghavachari, J. S. Binkley, C. González, R. L. Martin, D. J. Fox, D. J. Defrees, J. Baker, J. J. P. Stewart, and J. A. Pople, *Gaussian 92 (Revision E.2)*, Gaussian, Inc., Pittsburgh, PA, 1992.
42. P. J. Flory, *Statistical Mechanics of Chain Molecules*, Interscience, New York, 1969.